Electron to selectron pair conversion in a supersymmetric bubble with jet production by Bose enhancement

L. Clavelli* and I. Perevalova†

Department of Physics and Astronomy, University of Alabama, Tuscaloosa Alabama 35487, USA
(Received 4 October 2004; published 7 March 2005)

In the standard model, energy release in dense stars is severely restricted by the Pauli exclusion principle. However, if, in regions of space of high fermion degeneracy, there is a phase transition to a state of exact supersymmetry (SUSY), fermion to sfermion pair conversion followed by radiative transitions to the Bose ground state could lead to a highly collimated gamma ray burst. We calculate the cross section for $ee \to \tilde{e}\,\tilde{e}$ in a SUSY bubble and construct a monte carlo for the resulting sfermion amplification by stimulated emission.

DOI: 10.1103/PhysRevD.71.055001 PACS numbers: 11.30.Pb, 12.60.Jv, 13.66.–a, 13.66.Lm

I. INTRODUCTION

Recently it has been proposed that the puzzling gamma ray bursts seen over the last few decades in satellite observations [1] could be due to a transition to the SUSY vacuum in compact astrophysical objects such as white dwarf or neutron stars [2]. This phase transition could be catalyzed by the high matter density of such stars and, once nucleated, will spread through the entire star. Such a catalysis has been demonstrated in low dimensional models [3] at high density and is probably a feature of dense matter in arbitrary dimensions [4].

In such a SUSY bubble, normal particle pairs can convert to sparticle pairs, which, being bosons, can drop to the ground state through gamma ray emission. In this way, the entire kinetic energy of a degenerate fermi sea can be radiated away. It is possible that the high degree of collimation observed in the gamma ray bursts could be due to Bose enhancement as is familiar in terrestrial lasers. If this transition occurs in white dwarf stars, there will be a multicomponent structure to the bursts as various particle species convert to their SUSY partners, possibly interrupted by periods of fusion of supersymmetric nuclei. A more complete discussion of the physical picture proposed is contained in [2]. This model is dependent on the assumption that the common particle and sparticle mass in the exact SUSY phase is equal to (or less than) the particle mass in the broken-SUSY phase. This mild though necessary assumption is, perhaps, supported by the string theory result that the ground state supermultiplets are of low (in fact zero) mass.

The possibility of a phase transition between vacua requires that the vacuum structure of the theory is dynamically determined as in string theory and in certain other models of SUSY breaking. The other possibility, that the SUSY breaking is determined by arbitrary fixed parameters as in the minimal supersymmetric standard model is probably less satisfying from a theoretical perspective. The transition we consider (from an unstable de Sitter vacuum with positive vacuum energy to a stable SUSY vacuum) has been considered in the formal string theory study of Ref. [5] although phenomenological consequences are not part of that work.

In this article we treat the simplest component of the phase transition, namely, the conversion of electron to selectron pairs.

$$e^-(p_1)e^-(p_2) \to \tilde{e}^-(p_3)\tilde{e}^-(p_4) \tag{1.1}$$

This cross section was calculated previously in [6] neglecting the electron mass as appropriate in the broken-SUSY phase where the electron mass is many orders of magnitude less than the selectron mass. In the exact SUSY phase the electron and selectron masses are equal and the cross section near threshold is needed. The corresponding simple extensions of the cross section formulae are given in Sec. II. The results are applicable to a possible SUSY conversion in a white dwarf which, in the broken-SUSY phase, is stable against gravitational collapse due to the electron degeneracy. In a neutron star, the SUSY conversion would be more complicated and the energy release would be more slow since sneutrons will not efficiently radiate. Even in the white dwarf case, nuclear processes may be somewhat more important than the electron component which we treat here. In Sec. III, we use the cross section of (1.1) in an event generator for the differential transition rate incorporating the Bose enhancement effect. We assume that the entire kinetic energy of the selectrons is released into gamma radiation as the scalars drop into the ground state although we do not treat the radiative processes explicitly in this paper. Section IV is reserved for a summary of our conclusions.

II. CROSS SECTION CALCULATION

In the process $e^-e^- \to \tilde{e}\,\tilde{e}$ the mediator of the interaction is a Majorana spinor $\tilde{\gamma}$ as shown in Fig. 1.

We follow the Feynman rules as reviewed in [7]. In particular the vertex factor for an incoming left (right)

*E-mail address: lclavell@bama.ua.edu
†E-mail address: perev001@bama.ua.edu

 © 2005 The American Physical Society

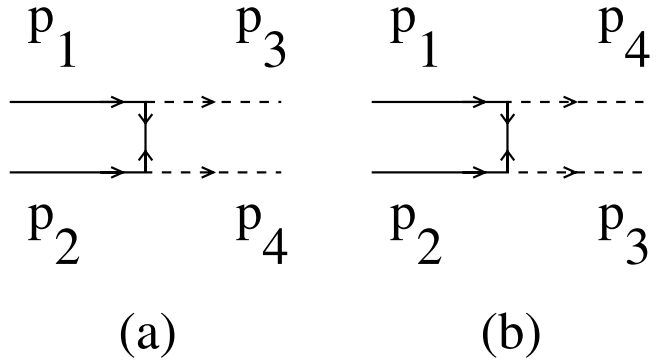

FIG. 1. Feynman graphs for the conversion of an electron pair to selectrons, Eq. (1.1), via photino exchange .

handed Dirac fermion of spinor index β, an outgoing SUSY partner, and an outgoing Majorana fermion of spinor index α is

$$-ie\sqrt{2}\quad\frac{(1\mp\gamma_5)_{\alpha\beta}}{2} \tag{2.1}$$

and for a Majorana fermion line with double incoming arrows as in Fig. 1 carrying momentum q from this vertex to one where the Majorana fermion is emitted with index γ, the propagator is

$$i\frac{[C^{-1}(\not{q}+m)]_{\alpha\gamma}}{q^2-m^2+i\epsilon}. \tag{2.2}$$

Acting on the Dirac spinor the charge conjugation operator, C, has the effect

$$u^T(p,s)C^{-1}=-\overline{v}(p,s). \tag{2.3}$$

For the associated production of left and right selectrons, the amplitudes corresponding to graphs a and b in figure one are then

$$\begin{aligned}M_a&=\frac{ie^2}{2(t-M_{\tilde\gamma}^2)}u^T(p_1)(1+\gamma_5)^TC^{-1}\\&\quad\times(\not{p}_1-\not{p}_3+M_{\tilde\gamma})(1-\gamma_5)u(p_2)\\M_b&=\frac{ie^2}{2(u-M_{\tilde\gamma}^2)}u^T(p_1)(1-\gamma_5)^TC^{-1}\\&\quad\times(\not{p}_1-\not{p}_4+M_{\tilde\gamma})(1+\gamma_5)u(p_2).\end{aligned}$$

Here and throughout the paper the Mandelstam variables are

$$s=(p_1+p_2)^2\qquad t=(p_1-p_3)^2\qquad u=(p_1-p_4)^2.$$

The squared matrix elements take the form:

$$\begin{aligned}|\mathcal{M}_{LR}|^2&=\Sigma_{ss'}(M_aM_a^\dagger+M_bM_b^\dagger+M_aM_b^\dagger+M_bM_a^\dagger)\\&=e^4\Big\{\frac{1}{(t-M_{\tilde\gamma}^2)^2}[ut-2tm_e^2-(m_{\tilde e}^2-m_e^2)^2]\\&\quad+t\leftrightarrow u+\frac{4m_e^2(m_{\tilde e}^2-m_e^2)}{(t-M_{\tilde\gamma}^2)(u-M_{\tilde\gamma}^2)}\Big\}\end{aligned} \tag{2.4}$$

where $\Sigma_{ss'}$ denotes averaging over the spins of incoming particles. The production of two left or two right selectrons is obtained from the above by the appropriate changes in the helicity projection operators and dividing by the statistical factor for the identical final state particles.

$$\begin{aligned}|\mathcal{M}_{RR}|^2&=|\mathcal{M}_{LL}|^2\\&=\frac{e^4M_{\tilde\gamma}^2}{2!}(s-2m_e^2)\Big(\frac{1}{t-M_{\tilde\gamma}^2}+\frac{1}{u-M_{\tilde\gamma}^2}\Big)^2.\end{aligned} \tag{2.5}$$

In the limit of negligible electron mass, these agree with the spin-averaged formulas of [7] and with the squared helicity ampltudes of [6]. Other authors have considered the effect of other neutralino exchanges [8,9] but, since these particles in the SUSY phase have masses comparable to the W and Z, they are negligible for our purposes.

In the numerical calculations of Section III, we will need the integrated matrix elements squared:

$$f_{AB}(s)=\frac{1}{\sqrt{s(s-4m^2)}}\int_{4m^2-s}^{0}dt|\mathcal{M}_{AB}|^2. \tag{2.6}$$

The total cross sections are related to the f_{AB} by

$$\sigma_T(ee\to\tilde e_A\tilde e_B)=\frac{f_{AB}(s)}{16\pi\sqrt{s(s-4m^2)}}. \tag{2.7}$$

Calculations for the different Matrix elements in the SUSY phase ($m_e=m_{\tilde e}=m$) will give us the following:

$$\begin{aligned}f_{LR}(s)&=2e^4\sqrt{\frac{s-4m^2}{s}}\Big(\frac{-2s-2M_{\tilde\gamma}^2+6m^2}{s-4m^2+M_{\tilde\gamma}^2}\\&\quad+\frac{s-2m^2+2M_{\tilde\gamma}^2}{s-4m^2}\ln\frac{s-4m^2+M_{\tilde\gamma}^2}{M_{\tilde\gamma}^2}\Big)\\f_{LL}(s)&=f_{RR}(s)\\&=\frac{4e^4(s-2m^2)}{\sqrt{s(s-4m^2)}}\Big(\frac{s-4m^2}{(s-4m^2+M_{\tilde\gamma}^2)}\\&\quad+\frac{2M_{\tilde\gamma}^2}{s-4m^2+2M_{\tilde\gamma}^2}\ln\frac{s-4m^2+M_{\tilde\gamma}^2}{M_{\tilde\gamma}^2}\Big).\end{aligned}$$

These are only logarithmically sensitive to the photino mass. The selectron momentum and angular distributions to be calculated in the next section are even less sensitive to the photino mass since they depend only on the shape of the cross sections and not on the absolute values. Integrals

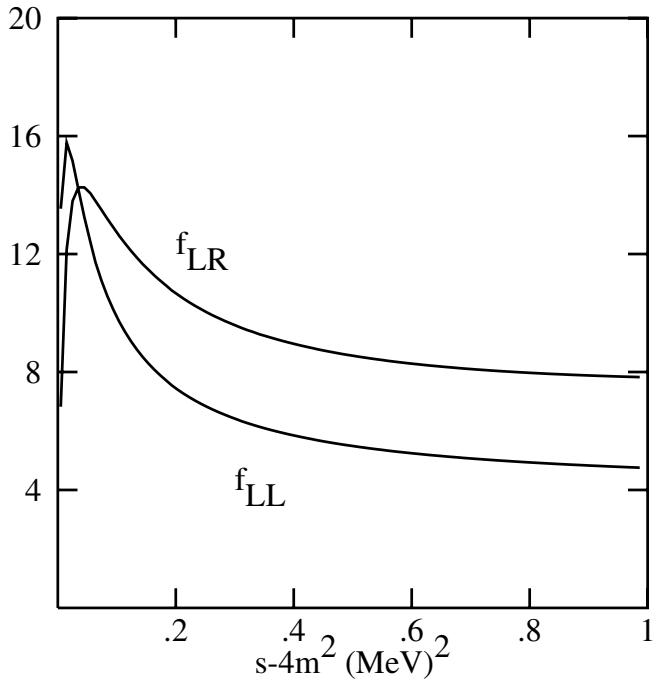

FIG. 2. Behavior of the t integrated matrix elements squared as a function of $s - 4m^2$.

of f_{LL} and f_{LR} as required in the conversion rates discussed in the next section are finite in the limit of zero photino mass. However, a more precise treatment of photino mass effects requires a careful treatment of experimental resolution beyond the scope of this study. The behavior of the functions $f_{LL}(s)$ and $f_{LR}(s)$ for $M_{\tilde{\gamma}} = m/4$ is shown in figure 2. For larger values of the photino cutoff mass, f_{LR} lies below f_{LL} although the near constant values of the two $f's$ well above threshold are not affected.

III. EVENT GENERATION

In a typical white dwarf (solar mass and earth radius) there are

$$N_0 = 6 \cdot 10^{56} \tag{3.1}$$

electrons in a degenerate Fermi sea:

$$dN = \frac{2p^2 dp \quad d[cos(\theta)] \quad d\phi}{(2\pi\hbar)^3}. \tag{3.2}$$

The Fermi momentum is

$$p_{\max} = \left(\frac{3N}{8\pi V}\right)^{1/3} 2\pi\hbar = 0.498\left(\frac{n}{n_0}\right)^{1/3} \mathrm{MeV}/c. \tag{3.3}$$

Here n is the electron number density and n_0 is that of the nominal white dwarf of solar mass and earth radius. The event rate for process (1.1) in a volume V is given in terms of the differential cross section by

$$\Gamma = \int d\sigma \left(\frac{dN_i v_i}{V}\right) dN_t, \tag{3.4}$$

where the incident and target distributions are given by (3.2). The differential cross section is given in terms of the invariant matrix element squared by

$$d\sigma = \frac{\mid \mathcal{M} \mid^2 d\Omega_f}{4E_1 E_2 v}. \tag{3.5}$$

Here m is the common electron and selectron mass in the SUSY bubble. The energies, E_i and the incident velocity, v, are those of the target rest frame. The final state phase space is

$$d\Omega_f = \frac{d^3p_3}{2E_3}\frac{d^3p_4}{2E_4}\frac{\delta^4(p_1 + p_2 - p_3 - p_4)}{(2\pi)^2} \tag{3.6}$$

where any statistical factors that occur for identical final state particles are put into the matrix element squared. Thus the Lorentz invariant event rate per unit volume is

$$\frac{d\Gamma}{V} = \frac{4 \mid \mathcal{M} \mid^2}{(2\pi)^8}\frac{d^3p_1}{2E_1}\frac{d^3p_2}{2E_2}\frac{d^3p_3}{2E_3}\frac{d^3p_4}{2E_4} \times \delta^4(p_1 + p_2 - p_3 - p_4). \tag{3.7}$$

The p_2 integral can be done trivially using the δ function and the p_1 integral is then conveniently done in the CM frame with $\hat{p}_3 = \hat{e}_z$.

$$\frac{d^3p_1}{2E_1}\delta[(p_3 + p_4 - p_1)^2 - m^2] = \frac{\pi dt}{2\sqrt{s(s-4m^2)}}. \tag{3.8}$$

Thus

$$\frac{d\Gamma}{V} = \frac{\mid \mathcal{M} \mid^2}{(2\pi)^7\sqrt{s(s-4m^2)}} dt \frac{d^3p_3}{2E_3}\frac{d^3p_4}{2E_4} \tag{3.9}$$

or

$$\frac{d\Gamma}{V} = \frac{\mid \mathcal{M} \mid^2}{(2\pi)^7\sqrt{s(s-4m^2)}} dt \frac{p_3^2}{2E_3} \times \frac{p_4^2}{2E_4} dp_3 d\cos(\theta_3) d\phi_3 dp_4 d\cos(\theta_4) d\phi_4. \tag{3.10}$$

For $p_{\max}$ we use the value of (3.3) corresponding to the Fermi energy in a white dwarf of earth radius and solar mass.

The final state of the process consists of two distinct species of scalars, $\tilde{e}_L$ and $\tilde{e}_R$. Thus the effective matrix element squared in (3.10) and elsewhere above is actually

$$\mid \mathcal{M} \mid^2 = \mid \mathcal{M}_{LR} \mid^2 + (\mid \mathcal{M}_{LL} \mid^2 + \mid \mathcal{M}_{RR} \mid^2). \tag{3.11}$$

In a bath of preexisting selectrons each matrix element squared is related to the elementary matrix element squared calculated with no preexisting selectrons by the Bose statistical factors

$$|\mathcal{M}|^2 = |\mathcal{M}_{0LR}|^2 [N_L(\vec{p}_3)+1][N_R(\vec{p}_4)+1] + (|\mathcal{M}_{0LL}|^2 [N_L(\vec{p}_3)+1][N_L(\vec{p}_4)+1] + |\mathcal{M}_{0RR}|^2 [N_R(\vec{p}_3)+1][N_R(\vec{p}_4)+1]). \quad (3.12)$$

The matrix elements of the previous section, calculated for the case of no selectrons in the initial state, are the $\mathcal{M}_0$ of this section. For the present we treat only the LL final state. The RR final state implies that there could be at least four gamma ray jets in each burst and possibly many more if different energy levels in the Fermi sea lead to independent gamma ray bursts. This suggests a picture where the gamma ray jets are much more numerous in each stellar explosion and, individually, much more narrow and less energetic than currently assumed. A more detailed analysis, beyond the scope of the current paper, is needed to explore this point but we speculate that this could be the cause of the ''spikey'' nature or rapid time variability of many of the observed bursts.

Our remaining analysis in this paper, restricted to the LL jets, allows us to drop, the L subscript on the occupation numbers. The CM energy $\sqrt{s}$ is determined by $\vec{p}_3$ and $\vec{p}_4$. The t integral has been done analytically in Sec. II:

We define a grid of $N_{\rm bin}$ points in each of the six variables. In practice we choose $N_{\rm bin} = 15$. The discretized $i'th$ integration variable in (3.10) is

$$v_i = v_{i,\min} + (v_{i,\max} - v_{i,\min})(N_i + 1/2)/N_{\rm bin} \quad (3.13)$$

where

$$0 \le N_i \le N_{\rm bin} - 1. \quad (3.14)$$

In order to generate events with probability defined by (3.10) and (3.12), it is convenient to linearize the six dimensional integral. We define the composite integer variable

$$j = \sum_{i=1}^{6} N_{\rm bin}^{6-i} N_i \quad (3.15)$$

with limits

$$0 \le j \le N_{\rm bin}^6 - 1. \quad (3.16)$$

Each value of j corresponds to a unique value of each of the six integration variables. The distribution of events is then defined as an integer valued array with $N_{\rm bin}^6$ grid points. To handle 15^6 grid points requires careful memory management techniques. [1] The integer j can be decomposed into two integers j_3 and j_4 which encode the three dimensional vectors $\vec{p}_3$ and $\vec{p}_4$, respectively.

$$j_3 = j/N_{\rm bin}^3 \qquad j_4 = j \bmod N_{\rm bin}^3 \qquad j = N_{\rm bin}^3 j_3 + j_4. \quad (3.17)$$

The first of these equations is defined by integer division, i.e., j_3 is the largest integer less than or equal to $j/N_{\rm bin}^3$. The event generation follows standard techniques [10] except that the probability distribution changes with each event due to the Bose enhancement factors. In the event generation of the selectron distributions, constant overall factors in (3.10) play no role. We begin by putting all the selectron occupation numbers to zero and calculating the (unnormalized) probabilities

$$P(j) = f_{LL}(s)\frac{p_3^2 p_4^2}{E_3 E_4}[N(j_3)+1][N(j_4)+1]. \quad (3.18)$$

We then define the partial sum

$$R(j) = \sum_{i=0}^{j} P(i) \quad (3.19)$$

as well as the complete sum

$$P_{\rm int} = \sum_{i=0}^{N_{\rm bin}^6 - 1} P(i). \quad (3.20)$$

$R(j)$ is a monotonically increasing function of j. One then calls a random number w between zero and one. For the unique value of j for which $w > R(j-1)/P_{\rm int}$ and $w \le R(j)/P_{int}$ one increments the selectron occupation numbers by one:

$$N(j_3) \to N(j_3) + 1, \qquad N(j_4) \to N(j_4) + 1. \quad (3.21)$$

$P(j\prime)$ changes in the jth bin only by a factor

$$f = [N(j_3)+1][N(j_4)+1]/[N(j_3)N(j_4)]. \quad (3.22)$$

Here $N(j_3)$ and $N(j_4)$ are the new occupation numbers (after incrementing). $R(j\prime)$ changes for each $j\prime \ge j$

$$R(j\prime) \to R(j\prime) + P(j)(f-1) \qquad for \qquad j\prime \ge j. \quad (3.23)$$

In addition

$$P_{\rm int} \to P_{\rm int} + P(j)(f-1). \quad (3.24)$$

After making these replacements, one adjusts $P(j)$:

$$P(j) \to P(j) f. \quad (3.25)$$

One then repeats the process as many times as possible choosing new random values of w. After very many events the distribution is amplified at two particular values of $\vec{p}_3$ and $\vec{p}_4$.

In the simulation two problems arise. The first is that the enhanced probability to put subsequent events in some particular $j'th$ bin is a very mild enhancement at first. Only after some huge number of events does the structure lock in on a particular j value. Since the number of available fermions in a compact star is of order 10^{56}, this is not a problem in principle but it does pose technical problems with computers of currently available speed and memory. To accelerate the buildup of jet structure, instead of incrementing the selectron occupation numbers by one

[1] We thank Doug Leonard for consultation on these techniques.

TABLE I. Selectron momentum and angular distributions showing the effect of boson enhancement. In this run the occupation numbers are incremented by two at each throw of the dice.

p (MeV)	N(p)	$\cos\theta$	N($\cos\theta$)	ϕ	N(ϕ)
0.017	42	−0.93	60914	0.209	16692
0.050	360	−0.80	87034	0.628	56060
0.083	986	−0.67	41284	1.047	94394
0.116	1948	−0.53	28832	1.466	30174
0.149	3178	−0.40	14672	1.885	63792
0.183	4690	−0.27	24064	2.304	127048
0.216	6572	−0.13	16452	2.723	607026
0.249	8410	0.00	52874	3.142	13538
0.282	11510	0.13	660320	3.560	50778
0.315	13548	0.27	16302	3.979	21316
0.349	17198	0.40	33942	4.398	46504
0.382	26284	0.53	112400	4.817	25394
0.415	63298	0.67	23458	5.236	13670
0.448	82526	0.80	23878	5.655	31868
0.481	1034494	0.93	78618	6.074	76790

at each throw of the dice, we increment by two. If one increments by more than one at each throw, the f of (3.22) has the obvious redefinition. The distributions in selectron momentum, polar angle cosine, and azimuthal angle after 600 000 throws (or 1.2 million events) is shown in Table I. The jagged polar angular distribution shown in Fig. 3 is an interesting feature of the calculation.

In a simplified run, (not shown here) where we look at the conversion of two electrons at the Fermi surface,

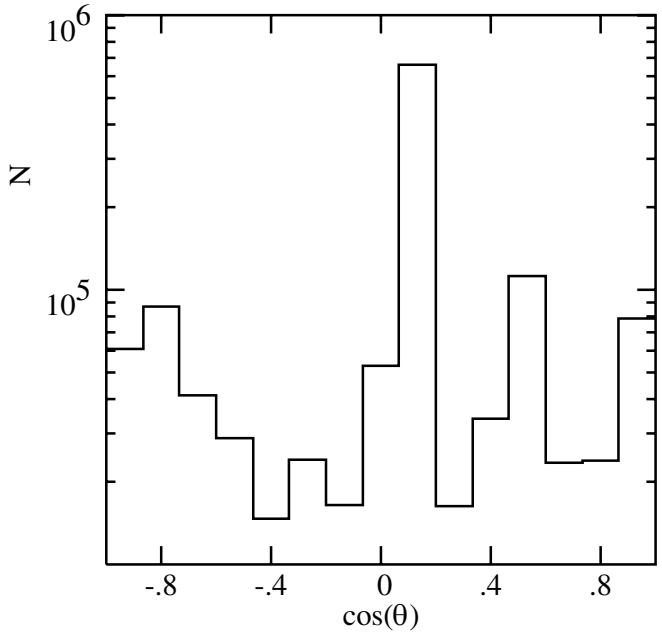

FIG. 3. angular distribution after 600 000 throws, showing effect of Bose enhancement. In this run, the bins are incremented twice at each throw

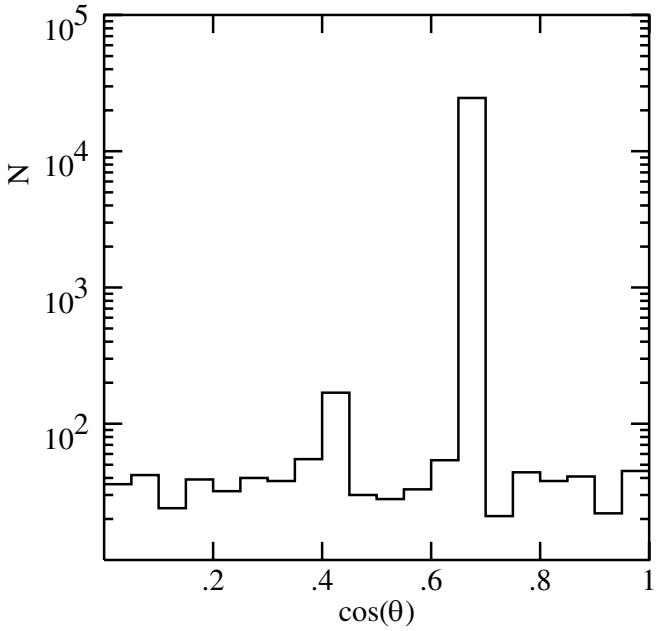

FIG. 4. Polar angle distribution for conversion of those electron pairs whose center of momentum is that of the star. One quadrant of the angular space is shown with a balancing selectron jet in the opposite direction.

although there are no observable jets in the first million events, a clear jet structure emerges at $9 \cdot 10^7$ events even when selectron occupation numbers are incremented by one at each event as is physically required. In this run it is not required that the electron pair has zero total momentum in the rest frame of the star.

The second problem is the following. We have treated the star as having an inexhaustible supply of electrons of each momentum in the fermi sea. In practice this number is very large but not infinite. Only after all the electrons have been exhausted will the selectron momenta add to zero in the rest frame of the star. For the present one can artificially circumvent this problem by considering electron to selectron conversion among those electron pairs whose center of momentum frame is that of the star. Then we can choose one selectron according to the distribution of (3.10) with the other selectron necessarily having the balancing momentum. In this case we can rapidly see the jet structure develop incrementing each selectron occupation number by one at each throw of the dice. The corresponding selectron distribution is shown in Fig. 4 after only 50 000 events.

IV. CONCLUSIONS

The results after 600 000 throws of the dice are shown in Table I. Since the integrated squared matrix elements vanish at threshold and the phase space element favors high momenta, the typical selectron momentum is thus somewhat greater than the estimate in [2] based on the

average energy in the electron Fermi sea. The selectron momentum distributions given in Table I will more or less directly carry over into photon distributions since bosons will necessarily fall into the ground state via photon emission. Thus the firm prediction of MeV level photons in the burst is a quantitative, and perhaps the primary, result of the current paper. A secondary result is that, due to the increased production probability for higher photon energy (i.e., selectron kinetic energy in Table I), the initial spikes in a gamma ray burst would be expected to be of higher average photon energy than later components. This is consistent with observations [11]

The minimum duration of the burst was fixed in [2] by assuming that the SUSY bubble, once nucleated, would grow at the speed of light and that photons in the dense star would travel with effective index of refraction one. Both of these assumptions might need to be more closely examined.

In particular, since one should probably regard the bubble surface as a mechanical membrane, a more reasonable estimate of the burst duration might be given by assuming that the bubble expands at the speed of sound rather than the speed of light. Then, if one takes into account the range of masses and radii among white dwarfs and if one estimates the bubble expansion speed by the speed of sound in a star of corresponding average density, the range of predicted burst durations extends well into that of the observations. A detailed study of the duration distribution taking into account density inhomogeneities and other effects is a high priority subject of future study.

Finally, we should discuss our expectation that the SUSY bubble is confined to the dense star and does not escape to take over the universe. If one is in the false vacuum of broken-SUSY, bubbles of true vacuum (exact SUSY) are constantly being produced with a steeply falling distribution in bubble radius, r. At creation, or at any later stage in its development, a bubble of radius r will expand or contract depending on which behavior is energetically favorable. The condition for expansion depends on the surface tension, S, of the bubble and the energy density in the region immediately outside the bubble. Consider, for example, a bubble of exact SUSY in a larger region of broken-SUSY. Outside the bubble the energy density will be $\epsilon + \rho$ where ϵ is the vacuum energy and ρ is the outside ground state matter density if any. If the SUSY bubble were to make a virtual expansion into an infinitesimally larger spherical shell, its ground state energy density would be ρ_s. The difference between ρ and ρ_s is the excitation energy density of the electrons in the broken-SUSY phase. Classically, the ground state energy after such a virtual expansion minus the previous ground state energy is

$$\Delta E = \frac{4\pi}{3}[(r+\delta r)^3 - r^3](\rho_s - \rho - \epsilon) + 4\pi S[(r+\delta r)^2 - r^2] \tag{4.1}$$

or

$$\Delta E = -4\pi r \delta r[r(\epsilon + \Delta\rho) - 2S] \tag{4.2}$$

where we have put

$$\Delta\rho = \rho - \rho_s. \tag{4.3}$$

Classically therefore, the system will find it energetically advantageous to expand if $r > \frac{2S}{\epsilon+\Delta\rho}$. Similarly, the bubble will contract if its radius is below this density dependent critical value. A more exact instanton calculation [12] *in vacuo* ($\rho = \rho_s = 0$) replaces $2S$ by $3S$ in Eq. (4.2). One would, therefore, expect the critical radius for a SUSY bubble to be

$$R_c = \frac{3S}{\epsilon + \Delta\rho}. \tag{4.4}$$

In vacuo or ignoring the effect of the Pauli principle, $\Delta\rho = 0$. In a homogeneous region, if a bubble is created at greater than the critical radius, it will expand indefinitely. If however, the bubble comes to the boundary of a dense region outside of which ρ and $\Delta\rho$ are zero, the critical radius jumps discontinuously to its vacuum value, effectively confining the bubble to the high density region.

Given the indirect hints of supersymmetry from dark matter and accelerator experiments, given the positive vacuum energy suggested by the acceleration of the universe, and given the persistent suggestion of string theory that the true vacuum of the theory is supersymmetric, a phase transition from our broken-SUSY phase to the exact SUSY phase is probably inevitable. There are also good reasons to believe the transition to the true vacuum would be catalyzed in dense matter [4]. In addition, given the Bose nature of the final state particles, collimation due to stimulated emission is to be expected on physical grounds. Only our assumption that the probability of transition is sufficient in compact stars to reproduce the rate of gamma ray bursts might be considered speculative.

It is, however, clear that many points remain to be investigated in the current SUSY phase transition picture of gamma ray bursts. Some of these are:

(1) *calculation of the hadronic component of SUSY conversion.* This will become even more essential if the bursts originate in Neutron stars and not in white dwarfs.
(2) *calculation of the gamma ray spectrum* from radiative SUSY conversion and (not independent) bremstrahlung from the final state selectron gas. Since the selectrons are bosonic, all of their kinetic energy will emerge as photons.
(3) *depletion effects in the Fermi sea*
(4) *fusion of SUSY (or partially SUSY) nuclei.* This could lead to temporary interruption of the gamma ray bursts.
(5) *polarization effects*

Only after many of these effects have been studied can one attempt to predict the angular width of jets, the energy spectra, the ''light curves'', and other features of the rapidly growing observational data. As shown here and in [2] the SUSY phase transition model provides a framework for discussing other details of this phenomenon that is alternative to the more traditional astrophysical approaches. These latter approaches based on relativistic ejection of large bodies of neutral matter from black hole accretion disks with the subsequent conversion of a large amount of kinetic energy into collimated gamma rays on subsecond time scales attempt to describe gamma ray bursts within the boundaries of standard model physics but have not as yet led to sharp predictions for typical photon energies or total burst energies untied to free parameters in the models. In addition the physical basis of the energy release (central engine) or the mechanism for production of collimated gamma rays are not yet as fully defined in the accretion models as in the current phase transition model. For recent papers marking the current status of traditional astrophysical approaches and giving references to earlier work along those lines see [13,14].

Another important area that needs study is the possible role of a SUSY phase transition in supernova collapse. This is potentially of great interest since it has become apparent in recent years that the current standard model of supernova explosion (energy deposited by neutrinos in a surrounding shell of matter) is not effective in producing the observed explosions [15,16]. This problem might also raise questions about the efficiency of $\nu\overline{\nu}$ annihilation into an e^+e^- cloud available for production of a relativistic fireball to explain gamma ray bursts as suggested in [13].

Examples of other new physics suggestions for gamma ray bursts can be found in [17] and references contained therein. Again, it seems that these models might not have the same success in predicting the salient features of gamma ray bursts as does the SUSY phase transition model.

ACKNOWLEDGMENTS

This work was supported in part by the U. S. Department of Energy under grant DE-FG02-96ER-40967. We gratefully acknowledge discussions with Doug Leonard, Phil Hardee, Bill Keel, George Karatheodoris, and Wai-Yee Keung.

[1] Bing Zhang and Peter Mészáros, Int. J. Mod. Phys. A **19**, 2385 (2004).
[2] L. Clavelli and G. Karatheodoris, hep-ph/0403227.
[3] A. S. Gorsky and V. G. Kiselev, Phys. Lett. B **304**, 214 (1999).
[4] M. B. Voloshin, Phys. Rev. D **49**, 2014 (1994).
[5] S. Kachru, R. Kallosh, A. Linde, and S. Trivedi, Phys. Rev. D **68**, 046005 (2003).
[6] W.-Y. Keung and L. Littenberg, Phys. Rev. D **28**, 1067 (1983).
[7] H. E. Haber and G. L. Kane, Phys. Rep. **117**, 75 (1985).
[8] F. Cuypers, G. van Oldenborgh, and R. Ruckl, Nucl. Phys. **B409**, 128, (1993).
[9] J. Feng and M. Peskin, Phys. Rev. D **64**, 115002 (2001).
[10] See the summary of Monte Carlo techniques in Review of Particle Properties, Particle Data Group, Phys. Rev. D **66**, 010001 (2002).
[11] E. Pian *et al.* (to be published).
[12] S. Coleman, Phys. Rev. D **15**, 2929 (1977); C. G. Callan and S. Coleman, Phys. Rev. D **16**, 1762 (1977); S. Coleman and Frank DeLuccia, Phys. Rev. D **21**, 3305 (1980).
[13] W. H. Lee, E. Ramirez-Ruiz, and D. Page, Astrophys. J. **608**, L5 (2004).
[14] R. Yamazaki, K. Ioka, and T. Nakamura, Astrophys. J. **607**, L103 (2004).
[15] Huaiyu Duan, Phys. Rev. D **69**, 123004 (2004).
[16] H. A. Bethe, Rev. Mod. Phys. **62**, 801 (1990).
[17] R. Ouyed and F. Sannino, Astron. Astrophys. **387**, 725 (2002); R. Foot and Z. K. Silagadze, astro-ph/0404515.